

Using developmental dynamics for evolutionary prediction and control

Lisandro Milocco^{1,*}

Tobias Uller^{1,†}

1. Department of Biology, Lund University, Lund, Sweden

* lisandro.milocco@biol.lu.se; ORCID: 0000-0003-3953-0407

† ORCID: 0000-0003-1293-5842

Manuscript elements: Abstract, Introduction, Results, Discussion, Conclusion, Materials and Methods, 4 Main Figures, 2 Appendices, References, 2 Supplementary Figures.

Keywords: evo-devo, plasticity, evolvability, dynamical systems

1 **Abstract**

2 Understanding, predicting, and controlling the phenotypic consequences of genetic and environmen-
3 tal change is essential to many areas of fundamental and applied biology. In evolutionary biology,
4 the generative process of development is a major source of organismal evolvability that constrains
5 or facilitates adaptive change by shaping the distribution of phenotypic variation that selection can
6 act upon. While the complex interactions between genetic and environmental factors during devel-
7 opment may appear to make it impossible to infer the consequences of perturbations, the persistent
8 observation that many perturbations result in similar phenotypes indicates that there is a logic to
9 what variation is generated. Here, we show that a general representation of development as a dy-
10 namical system can reveal this logic. We build a framework that allows to predict the phenotypic
11 effects of perturbations, and conditions for when the effects of perturbations of different origin are
12 concordant. We find that this concordance is explained by two generic features of development,
13 namely the dynamical dependence of the phenotype on itself and the fact that all perturbations
14 must be funneled by the same developmental process. We apply our theoretical results to classi-
15 cal models of development and show that it can be used to predict the evolutionary response to
16 selection using information of plasticity, and to accelerate evolution in a desired direction. The
17 framework we introduce provides a way to quantitatively interchange perturbations, opening a new
18 avenue of perturbation design to control the generation of variation, and thus evolution.

19 Introduction

20 A complete theory of organismal evolution requires a theory of phenotypic variation, a theory of
21 natural selection, and a theory of heredity. While tremendous advances have been made in the last
22 century to understand the two latter pillars of Darwinian evolution, a theory for the generation of
23 phenotypic variation remains elusive.

24 The process that generates variation in morphology, physiology, and behavior is known as
25 development in the broad sense (Gilbert and Barresi 2016). Notoriously complex and non-linear
26 interactions between genes, cells, tissues and environmental factors during development make it
27 difficult to grasp the phenotypic consequences of genetic and environmental perturbations. Indeed,
28 the diversity and complexity of developmental systems could be taken as evidence that *a priori*
29 inference of the consequences of perturbations rarely will be feasible. A pessimistic conclusion is
30 therefore that the best one could hope for is to demonstrate that generative processes in principle
31 can impact evolutionary trajectories (Rice 2002, Morrissey 2015, Gonzalez-Forero 2023), while
32 studies that demonstrate *how* development affects evolution will remain a collection of idiosyncratic
33 case studies (Beldade et al. 2002, Brakefield 2006, Galis et. al 2010). This perception that
34 generative processes are intrinsically unpredictable, and that selection is the only reliable force in
35 evolution is also reflected in biotechnology and medicine, where attempts to direct evolutionary
36 processes emphasize control over selective regimes rather than control over generative processes.

37 In this paper, we provide a more optimistic perspective by addressing a particular problem
38 concerning the generation of variation, and its implications for evolution: the relationship between
39 the phenotypic effects of genetic and environmental perturbation. Genetic and environmental
40 effects on phenotypic variation have often been considered independent, as implicitly assumed when
41 environmental effects are modelled as the uncorrelated residuals of a linear regression of phenotype
42 on genotype in quantitative genetics (Lynch and Walsh 1998). However, since both genetic and
43 environmental perturbations are channeled through the same developmental system, it is unlikely
44 that this assumption generally holds true (Cheverud 1988, West-Eberhard 2003). It is indeed well

45 known that environmental change occasionally induces phenotypes that resemble genetic mutants
46 (e.g., melanism in butterflies, Nijhout 1984) and it has been shown that plastic responses are biased
47 towards phenotype dimensions with high additive genetic variation (Noble et al. 2019), but the
48 existing body of work is mostly a collection of empirical observations.

49 If genes and environments are equivalent, or interchangeable, as sources of phenotypic variation,
50 this could have important consequences for understanding and predicting evolution, and eventually
51 controlling it. In particular, gene-environment interchangeability implies that there is a formal con-
52 nection between evolvability and plasticity. Evolvability can be defined as the capacity to generate
53 phenotypic variation in response to genotypic variation (Kirschner and Gerhart 1998), while plas-
54 ticity refers to the same capacity for phenotypic variation in response to environmental variation.
55 If genetic and environmental perturbations are interchangeable, the evolution of plasticity may
56 shape evolvability and *vice versa*, and information of one can reveal features of the other (Chevin
57 et al. 2022). Previous theoretical work has suggested that such a relationship between plasticity
58 and evolvability does exist (Wagner and Altenberg 1996, Ancel and Fontana 2000, Espinosa-Soto
59 et al. 2011, Draghi and Whitlock 2012, Furusawa and Kaneko 2015, van Gestel and Weissing 2016,
60 Brun-Usan et al. 2021), but there is no general framework to explicitly define the conditions for
61 when this relationship should be expected, or to study its evolutionary implications. Such under-
62 standing would enable the design combinations of perturbations to drive the developmental system
63 to a desired state, thus controlling the generation of variation.

64 The aim of this paper is to introduce a conceptual framework to understand when genetic and
65 environmental perturbation will cause shifts in phenotype in similar directions in trait space. We
66 illustrate this phenomenon of alignment using *in silico* experiments of reaction diffusion models and
67 gene regulatory networks. We show how the theory can be used (i) to predict the concordance of
68 phenotypic effects of perturbations of different origins, (ii) to estimate the effects of mutations on the
69 phenotype, (iii) to infer evolvability using information of plasticity, and (iv) to accelerate evolution
70 in a desired direction. This ability to convert information from plastic responses into information
71 about evolutionary potential, and vice versa, could have applications in diverse areas concerned

72 with the phenotype, including developing solutions to environmental and societal challenges using
73 biotechnological engineering.

74 **Results**

75 The results are presented in sections. First, we introduce a general representation of development
76 as a dynamical system. Second, we develop the formalism to study the phenotypic effect of a
77 single perturbation. Third, we study the alignment between perturbations of different origins (e.g.,
78 genetic and environmental). Finally, we apply the theoretical framework to classical models of
79 development, namely reaction-diffusion models and gene regulatory networks, and show how it can
80 be used for evolutionary understanding, prediction and even control.

81 *A general representation of development as a dynamical system*

82 Mathematical models of development usually consist of a representation of the phenotype and a
83 set of rules of how this phenotype changes through developmental time, for example, through the
84 interaction among different components of the system. Examples of such models include reaction-
85 diffusion models (e.g., Kondo and Miura 2010), gene regulatory networks (e.g., Wagner 1994),
86 and models of morphogenesis (e.g., Salazar-Ciudad and Jernvall 2010). These models are com-
87 monly given mathematically as differential equations which are numerically integrated over time to
88 simulate a developmental trajectory, which is the change in the phenotypic values through devel-
89 opmental time. Following this body of work (Lewontin 1983, Alberch 1991), we take the general
90 representation of development given by:

$$91 \quad \dot{\mathbf{x}} = \mathbf{f}(t, \mathbf{x}, \boldsymbol{\lambda}), \quad \mathbf{x}(t_0) = \mathbf{x}_0 \quad (1)$$

92 where $\mathbf{x} = (x_1, x_2, \dots, x_n)$ is a vector composed of n variables that we refer to as *states*, with each
93 state x_i representing a different aspect of the phenotypes that is relevant to describe the systems
94 behavior through developmental time (e.g., the expression level of a given gene); $\dot{\mathbf{x}}$ is the time

95 derivative of \mathbf{x} , which gives the temporal change in the states; t is developmental time; \mathbf{f} is a
96 developmental function determining the rules of how the states change in time; \mathbf{x}_0 are the state
97 values at initial time t_0 , known as the initial conditions; and $\boldsymbol{\lambda} = (\lambda_1, \lambda_2, \dots, \lambda_p)$ are developmental
98 parameters, which can be genetic or environmental (e.g., the affinity of a cofactor modulating
99 downstream gene expression, or temperature during developmental time).

100 Equation (1) captures two central properties of development which will be important to derive
101 the results presented later. The first of these central aspects is that development depends at each
102 step on the preexisting phenotype. This is mathematically captured by the fact that the change in
103 the states at each time, given by $\dot{\mathbf{x}}$, is itself a function of the states \mathbf{x} at that time. This means that
104 the phenotype at any given time is both the effect of earlier and the cause of later developmental
105 changes. This feedback of the phenotype on itself makes development a *dynamical* phenomenon
106 rather than a *static* one (or *historical* rather than *programmatic*, Stent 1985, West-Eberhard 2003),
107 where the ways in which the phenotype can and cannot change at a given time depend on the state
108 of the phenotype at that time. Examples of this historicity of development include the sequential
109 determination of cell fate (Bassett and Wallace 2012) and sensitivity windows, where the same
110 perturbation results in a phenotypic effect only for responsive phenotypes at specific times during
111 development (Burggren and Mueller 2015).

112 The second important aspect of development highlighted by equation (1) is that changes in any
113 of the developmental parameters $\boldsymbol{\lambda}$ have an effect on the states \mathbf{x} through the same function \mathbf{f} .
114 In other words, any perturbation in the developmental parameters has to be channeled through
115 the same developmental pathways to result in a change in the states. As we show below, this
116 *funneling* (Cheverud 1988, West-Eberhard 2003) is fundamental for the alignment of the effects of
117 perturbations with different origins.

118 ***The effect of a perturbation on one developmental parameter***

119 We are interested in studying how a given developmental trajectory is affected by a perturbation
120 in one of the developmental parameters. We begin with a system with a single developmental

121 parameter (i.e., $\lambda = \lambda$), and we extend the results to multiple parameters later. Further, we will
122 assume that the developmental function \mathbf{f} is smooth, having continuous first partial derivatives.

123 The study of perturbations is always comparative: perturbations must be studied with respect to
124 an unperturbed reference. We thus need to define a reference developmental trajectory from which
125 to study deviations from. We define λ^* as the reference value for the developmental parameter (i.e.,
126 corresponding to an organism with the wild-type genotype in standard environmental conditions).
127 The developmental trajectory of the reference, unperturbed developmental system is thus given as
128 the unique solution of equation (1) for $\lambda = \lambda^*$, which we denote $\mathbf{x}(t, \lambda^*)$, as shown in Figure 1.

129 We are interested in the direction in which the reference developmental trajectory will change
130 when we introduce a small perturbation to λ^* . This type of study is known as *sensitivity analysis*
131 in dynamical systems theory (Khalil 2002). The direction of change is given by

$$132 \quad \mathbf{s}_\lambda(t) = \left. \frac{\partial \mathbf{x}(t, \lambda)}{\partial \lambda} \right|_{(t, \lambda^*)} \quad (2)$$

133 The vector $\mathbf{s}_\lambda(t)$ is known as the *sensitivity vector* (or *function*, Khalil 2002), and it is a vector of
134 length n containing the partial derivatives of the states x_1, x_2, \dots, x_n with respect to the parameter
135 λ , evaluated at the reference value λ^* and at time t . This vector then tells us how we expect
136 the states to change for a small change in the developmental parameter at each time t . For small
137 perturbations, we can predict the perturbed developmental trajectory using:

$$138 \quad \mathbf{x}(t, \lambda) \approx \mathbf{x}(t, \lambda^*) + \mathbf{s}_\lambda(t)(\lambda - \lambda^*), \quad (3)$$

139 which tells us that the perturbed developmental trajectory $\mathbf{x}(t, \lambda)$ will differ from the reference,
140 unperturbed trajectory $\mathbf{x}(t, \lambda^*)$ by an amount proportional to the difference $\lambda - \lambda_0$, with direction
141 determined by the vector $\mathbf{s}_\lambda(t)$. Equation (3) resembles a first order Taylor approximation, and is
142 only locally valid (i.e., for values of λ close to λ^*).

143 Calculating $\mathbf{s}_\lambda(t)$ is not straight-forward since we do not know the explicit relationship between
144 the states \mathbf{x} and the parameter λ . We show in *Appendix A* (see also Khalil 2002) that $\mathbf{s}_\lambda(t)$ can be

145 obtained as the the unique solution to

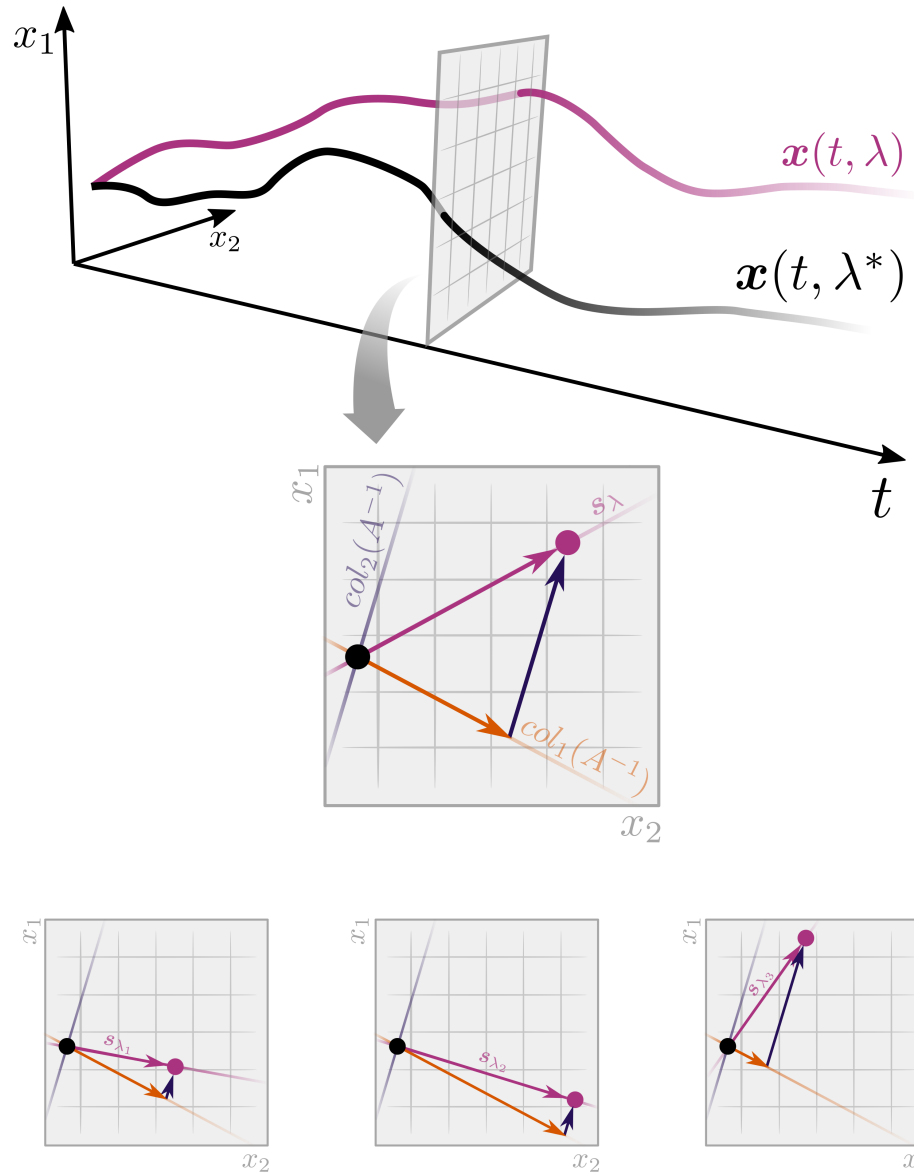
$$\begin{aligned}
 & \dot{\mathbf{s}}_\lambda(t) = A(t, \lambda^*)\mathbf{s}_\lambda(t) + \mathbf{b}_\lambda(t, \lambda^*), \quad \mathbf{s}_\lambda(t_0) = 0 \\
 146 \quad & A(t, \lambda^*) = \left. \frac{\partial \mathbf{f}(t, \mathbf{x}, \lambda)}{\partial \mathbf{x}} \right|_{\mathbf{x}(t, \lambda^*)}, \quad \mathbf{b}_\lambda(t, \lambda^*) = \left. \frac{\partial \mathbf{f}(t, \mathbf{x}, \lambda)}{\partial \lambda} \right|_{\mathbf{x}(t, \lambda^*)}
 \end{aligned} \tag{4}$$

147 The matrix $A(t, \lambda^*)$ is known as the Jacobian matrix and summarizes the relationship between
 148 \mathbf{f} and \mathbf{x} . Note that this Jacobian does not depend on what parameter λ is perturbed. The
 149 relationship between \mathbf{f} and λ is captured by the vector $\mathbf{b}_\lambda(t, \lambda^*)$. In this way, if we know the
 150 function \mathbf{f} , then we can calculate $A(t, \lambda^*)$ and $\mathbf{b}_\lambda(t, \lambda^*)$, and jointly solve numerically equations (1)
 151 and (4) to obtain $\mathbf{s}_\lambda(t)$, which is the vector of interest.

152 Under the assumption that the Jacobian is invertible, we can get the simplified expression

$$\begin{aligned}
 & \mathbf{s}_\lambda(t) = A^{-1}(t, \lambda^*) \underbrace{(\dot{\mathbf{s}}_\lambda(t) - \mathbf{b}_\lambda(t, \lambda^*))}_{\tilde{\mathbf{b}}_\lambda(t, \lambda^*)} \\
 153 \quad & = \text{col}_1(A^{-1})\tilde{b}_{\lambda,1} + \text{col}_2(A^{-1})\tilde{b}_{\lambda,2} + \dots + \text{col}_n(A^{-1})\tilde{b}_{\lambda,n}
 \end{aligned} \tag{5}$$

154 where $\text{col}_i(A^{-1})$ is the i -th column of $A^{-1}(t, \lambda^*)$ and $\tilde{b}_{\lambda,i}$ is the i -th element of vector $\tilde{\mathbf{b}}_\lambda$. This
 155 means that the sensitivity vector at a given time $\mathbf{s}_\lambda(t)$ can be expressed as a linear combination
 156 of the columns of $A^{-1}(t, \lambda^*)$ with weights determined by the elements of $\tilde{\mathbf{b}}_\lambda(t, \lambda^*)$. This result is
 157 shown graphically in Figure 1, and provides a basis to study alignment as explained in the next
 158 section. Note that $\tilde{\mathbf{b}}_\lambda(t, \lambda^*)$ reduces to $\mathbf{b}_\lambda(t, \lambda^*)$ if $\|\mathbf{b}_\lambda(t, \lambda^*)\| \gg \|\dot{\mathbf{s}}_\lambda(t)\|$, which is the case for an
 159 organisms that has reached steady state (e.g., adulthood).



160

Figure 1: A general framework to study the phenotypic effects of perturbations of different origins. On top, the reference developmental trajectory $\mathbf{x}(t, \lambda^*)$ in black and the perturbed trajectory $\mathbf{x}(t, \lambda)$ in purple through developmental time t . The panel in the middle shows that, at any given time, the effect of the perturbation on the trajectory, given by the sensitivity vector $\mathbf{s}_\lambda(t)$ is a linear combination of the columns of the matrix $A^{-1}(t, \lambda^*)$. The three panels at the bottom show the sensitivity vectors for different perturbations at a given developmental time are linear combinations of the columns of the same A^{-1} . \mathbf{s}_{λ_1} and \mathbf{s}_{λ_2} are largely aligned, but not \mathbf{s}_{λ_3} .

161 *Alignment between the effects of perturbations of different origin*

162 We now use the formalism introduced above to study the relationship between the phenotypic effects
163 of perturbations of different origins. Given two developmental parameters, we say that their effects
164 are totally aligned if the associated sensitivity vectors have an angle of 0° , meaning that the two
165 perturbations result in phenotypic changes in exactly the same direction. More generally, we say
166 that there is evidence of alignment if the two sensitivity vectors have an angle that is significantly
167 smaller, at a given confidence level, than the distribution of angles between independent random
168 vectors of the same dimension.

169 Figure 1 gives an example for three developmental parameters λ_1 , λ_2 and λ_3 , which can cor-
170 respond for example to the affinity of a cofactor modulating gene expression (genetic parameter),
171 temperature and salinity (environmental parameters), respectively. The effects of modifying each of
172 those parameters at time t is given by the vectors $\mathbf{s}_{\lambda_1}(t)$, $\mathbf{s}_{\lambda_2}(t)$ and $\mathbf{s}_{\lambda_3}(t)$, and the angles between
173 them determine alignment. From equation (5), we know that all of these sensitivity vectors can be
174 written as a linear combinations of the columns of the same matrix, the Jacobian $A^{-1}(t, \boldsymbol{\lambda}^*)$, where
175 each column is weighted by the elements of \tilde{b}_λ (note that we omit the arguments (t, λ^*) when it is
176 clear from context for readability). This provides sufficient conditions for alignment between the
177 effects of different perturbations; if two perturbations have a dominant component in the direction
178 of one of the columns of $A^{-1}(t, \boldsymbol{\lambda}^*)$ (i.e., $\tilde{b}_{\lambda,i} \gg \tilde{b}_{\lambda,j}$ for all $j \neq i$), then these perturbations will be
179 aligned.

180 The illustrative example in Figure 1 shows that $\mathbf{s}_{\lambda_1}(t)$ and $\mathbf{s}_{\lambda_2}(t)$ are largely aligned because
181 they both have a large component in the direction of the first column and a small component in the
182 direction of the second column of the Jacobian (i.e., $\tilde{b}_{\lambda_1,1} \gg \tilde{b}_{\lambda_1,2}$ and $\tilde{b}_{\lambda_2,1} \gg \tilde{b}_{\lambda_2,2}$). $\mathbf{s}_{\lambda_3}(t)$ is not
183 aligned with the other two vectors, since it has a large component in the second rather than first
184 column (i.e., $\tilde{b}_{\lambda_3,2} \gg \tilde{b}_{\lambda_3,1}$). We note that this sufficient condition is not necessary for alignment.
185 Indeed, there can be alignment according to our definition even if weights are not proportional
186 when the Jacobian has columns that are similar to each other.

187 The two components of the sensitivity vectors, namely $A^{-1}(t, \boldsymbol{\lambda}^*)$ and $\tilde{b}_{\lambda,i}$, are related to the two
188 key aspects of development highlighted by equation (1). The first of these aspects – the historicity
189 of development – is related to matrix $A^{-1}(t, \boldsymbol{\lambda}^*)$, the inverse of the Jacobian which summarizes the
190 relationship between \boldsymbol{f} and \boldsymbol{x} . This matrix determines the structure for phenotypic changes, since
191 its columns provide the directions in which the phenotype is able to respond to a perturbation.
192 These directions are independent of the nature of the perturbation itself and are determined by the
193 capabilities of the responsive phenotype at that time. The second relevant aspect of development
194 highlighted by equation (1) is the fact that all perturbations are funneled by the same developmental
195 function \boldsymbol{f} . This is related to the other component of the sensitivity vector, the weights $\tilde{b}_{\lambda,i}$. These
196 weights summarize the relationship between \boldsymbol{f} and $\boldsymbol{\lambda}$. If two developmental parameters affect the
197 same aspects of \boldsymbol{f} , then there will be alignment. However, if two parameters affect distinct aspects
198 of \boldsymbol{f} (e.g., they affect two different developmental modules) then we should not expect alignment
199 in general.

200 In the next sections, we apply this general framework to well-known models of development,
201 and use it to make evolutionary prediction and control.

202 *Alignment in a reaction-diffusion model*

203 Reaction–diffusion models are a set of models of pattern-formation that have been widely used
204 to represent diverse developmental processes, including digit formation and hair follicle placement
205 (Turing 1952, Sick et al. 2006, Kondo and Miura 2010, Green and Sharpe 2015). These models con-
206 sist of a physical representation of the tissue and a set of molecules called morphogens. Morphogens
207 diffuse and interact within the tissue, leading to the emergence of patterns as they accumulate in
208 specific spatial regions. Here, we will use one of these reaction-diffusion models known as the Gray-
209 Scott model (Gray and Scott 1990) to illustrate how we can study the alignment of phenotypic
210 effects of different origin using the framework introduced in the previous sections.

211 The developmental function \mathbf{f} for the Gray-Scott model is given by

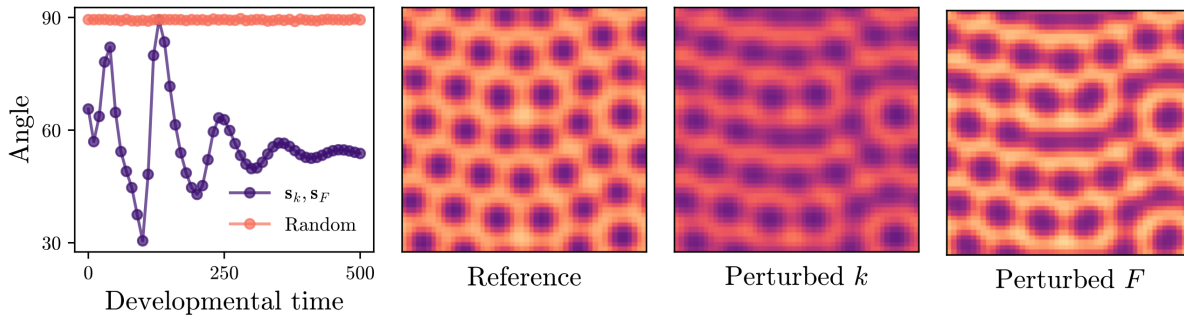
$$\begin{aligned} \dot{x}_1 &= D_1 \nabla^2 x_1 - x_1 x_2^2 + F(1 - x_1), \\ \dot{x}_2 &= D_2 \nabla^2 x_2 + x_1 x_2^2 - (F + k)x_2 \end{aligned} \tag{6}$$

213 where x_1 and x_2 are the cellular concentrations of morphogen 1 and 2, respectively, D_1 and D_2 are
214 their diffusion rates to neighboring cells, ∇^2 is the Laplacian operator, F is the production rate
215 of morphogen 1, and k is the rate of degradation of morphogen 2. We will study the alignment
216 between the phenotypic effects of perturbing the developmental parameters k and F .

217 We represent a portion of embryonic tissue as a grid of 50×50 cells (details of the simulations
218 are given in *Materials and Methods*). In each of these cells there is a given amount of the two
219 morphogens, so the total number of states in the system is $50 \times 50 \times 2 = 5000$. Diffusion of the
220 morphogens occurs between neighboring cells. The simulation is done for a window of time of
221 $t = 5000 \times h$ where $h = 0.1$ is the integration step. We start from initial conditions shown in
222 Supplementary Figure 1, and use the reference parameters values $D_1^* = 0.32$, $D_2^* = 0.06$, $k^* = 0.06$
223 and $F^* = 0.032$. We calculate $\mathbf{s}_k(t)$ and $\mathbf{s}_F(t)$ by jointly integrating equation (4).

224 Figure 2 shows that the angle between $\mathbf{s}_k(t)$ and $\mathbf{s}_F(t)$ remains around 50° . This means that
225 $\mathbf{s}_k(t)$ and $\mathbf{s}_F(t)$ are partially aligned, since this angle is significantly smaller than the angle between
226 random vectors of the dimension of the sensitivity vectors, which is 90° . This implies that the
227 phenotypic effects of perturbing k and F should be similar.

228 We test the analytical prediction of alignment by simulating perturbed systems. We run
229 simulations with small perturbations in the developmental parameters (i.e., $k = k^* + \Delta k$ and
230 $F = F^* + \Delta F$), and compare the resulting phenotypes. Figure 2 shows that the phenotypic effects
231 of either a decrease in k or an increase in F are largely aligned, resulting in the formation of *con-*
232 *nected dots* rather than *dots* as in the reference, unperturbed phenotype. Note that since the angle
233 between $\mathbf{s}_k(t)$ and $\mathbf{s}_F(t)$ is not 0° , we should not expect the perturbed phenotypes to be identical.



234

Figure 2: Alignment in a reaction-diffusion model. The panel on the left shows in purple the angle between $\mathbf{s}_F(t)$ and $\mathbf{s}_k(t)$ through developmental time, and in orange the average angle between $\mathbf{s}_k(t)$ and 10 random vectors of the same dimension (one standard deviation is also plotted but covered by the dots). The angle between \mathbf{s}_F and \mathbf{s}_k is significantly smaller than the angle between random vectors, indicating alignment between the phenotypic effects of perturbing k and F . The three panels to the right show the phenotypes, plotted as the concentration of morphogen 1 with higher concentration in lighter color, for the reference developmental parameters, perturbed k and F , respectively, at developmental time 500. As indicated by the small angle between \mathbf{s}_F and \mathbf{s}_k , the phenotypic effect of the perturbations is similar, resulting in *connected dots* as opposed to the *dotted* pattern in the reference.

235 *Alignment in a gene regulatory network*

236 We now use the general framework to study the alignment between the phenotypic effects of per-
 237 turbation with different origins in a gene regulatory network. In this section, we derive analytical
 238 results and test them using simulations. In the next section, we use the knowledge of alignment to
 239 connect plasticity and evolvability.

240 We use a common representation of gene regulatory networks found in the literature (Wagner
 241 1994, Draghi and Whitlock 2012, Brun-Usan et al. 2021), where the states are given by $\mathbf{x} =$
 242 (x_1, x_2, \dots, x_n) representing the expression levels of n transcription factors that regulate each other's
 243 expression. The function \mathbf{f} giving the change in the states during development for this example is

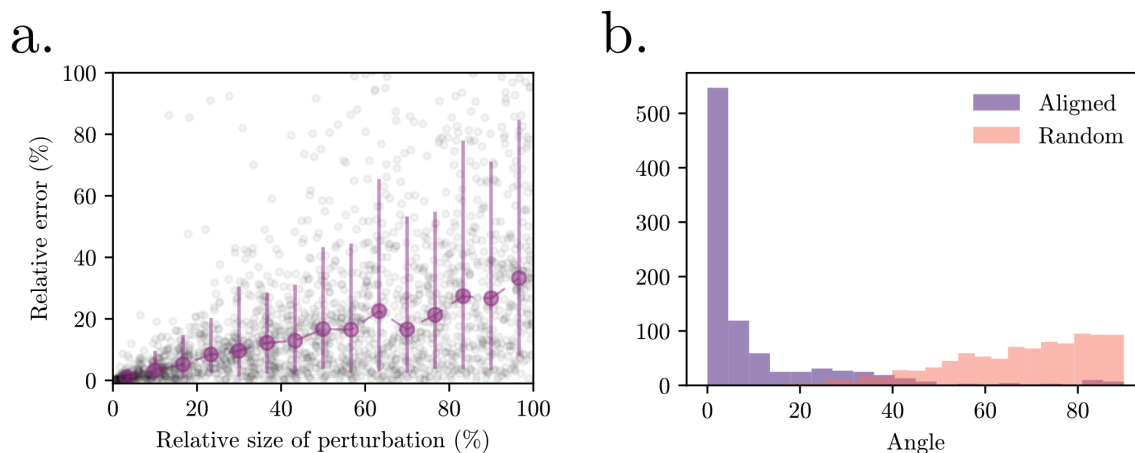
$$244 \quad \dot{x}_i = \frac{r(h_i)}{K_i + r(h_i)} - \mu_i x_i, \quad \text{with} \quad h_i = \sum_{j=1}^n \theta_{ij} x_j + u_i, \quad i = 1, 2, \dots, n \quad (7)$$

245 where θ_{ij} is the ij -th element of the matrix Θ , and gives the regulatory effect of gene j on the
 246 expression of gene i (i.e., $\theta_{ij} > 0$, $\theta_{ij} < 0$ and $\theta_{ij} = 0$ represent activation, inhibition and no
 247 interaction, respectively). The expression of each gene can also be activated or inhibited by envi-

248 ronmental inputs $\mathbf{u} = (u_1, u_2, \dots, u_n)$. Gene expression follows Michaelis-Menten dynamics with
249 coefficients K_i , and gene product has a degradation rate given by μ_i . In this way, the developmen-
250 tal parameters in this example are θ_{ij} , u_i , K_i and μ_i for all $i, j = 1, 2, \dots, n$. For the analyses in
251 this section and the next using the gene-regulatory network, we study the steady state, which we
252 consider maturity of the organism, where gene expression is no longer changing (i.e., $\dot{x}_i = 0$ for all
253 i). We use a bar to denote that a variable corresponds to the steady state (i.e., \bar{A} is the Jacobian
254 at the steady state).

255 In *Appendix B*, we obtain the Jacobian \bar{A} and the weights $\bar{\mathbf{b}}_\lambda$, for each of the developmental
256 parameters, and use them to calculate the sensitivity vector using equation (5). We find that for
257 a given i , the sensitivity vectors $\bar{\mathbf{s}}_{\theta_{ij}}$, $\bar{\mathbf{s}}_{u_i}$, $\bar{\mathbf{s}}_{K_i}$ and $\bar{\mathbf{s}}_{\mu_i}$ are always aligned (i.e., regardless of j)
258 since the weight vectors $\bar{\mathbf{b}}$ all have a non-zero value in the i -th position, and zeroes elsewhere. This
259 means that, for example, a perturbation in the environmental input u_i will result in a phenotypic
260 change that is in the same direction as a genetic change in any of the elements of the i -th row of
261 Θ . In particular, this phenotypic effect will occur in the direction of vector $\text{col}_i \bar{A}^{-1}$.

262 We test the analytical predictions by simulating gene networks of 5 genes and initial concen-
263 trations of 0.1 for all genes. We begin by using the sensitivity vectors to predict the phenotypic
264 effects of mutations, which are changes in the elements of the interaction matrix Θ . For this, we
265 generate 100 random gene regulatory networks each with a different reference interaction matrix
266 Θ_k^* . For each network k , we generate 20 mutants by modifying one element of Θ_k^* . We predict the
267 effect of these mutations using equation (3) as $\bar{\mathbf{x}}^* + \bar{\mathbf{s}}_{\theta_{ij}}(\theta_{ij} - \theta_{ij}^*)$, where $\bar{\mathbf{x}}^*$ is the steady state of
268 the unperturbed system and $\bar{\mathbf{s}}_{\theta_{ij}}$ is as obtained in *Appendix B*. We then compare this prediction
269 with the actual simulated steady state for the mutants.



270

Figure 3: The general framework predicts the effects of mutations and alignment with environmental perturbations. Panel a. shows the prediction error for the effect of a mutation using the sensitivity vector. The x -axis has the perturbation relative perturbation size $(\theta_{ij} - \theta_{ij}^*) / \theta_{ij}^*$. The relative error was calculated as the difference between predicted change using sensitivity vector and the simulated change, divided by the simulated change. 100 random networks were used as reference and 20 mutants were generated for each reference network. Panel b. shows the alignment between genetic and environmental perturbations in $\theta_{1,j}$ and u_1 for random j in $1, 2, \dots, 5$. The angle between the resulting changes was measured in degrees and plotted as a histogram in purple. Data includes 100 reference networks, each with 20 environmental and 20 genetic perturbations introduced. Orange histogram shows the angle between random vectors in 5-dimensional morphospace.

271 Figure 3.a. shows that the formalism based on sensitivity vectors predicts the effect of mutations
 272 on the phenotype. As expected, the error in the prediction goes to zero as the perturbations become
 273 smaller. Perturbations smaller than 20% in the parameters have median relative error smaller than
 274 3% in the prediction of their phenotypic effect. The predictions for this class of network is robust
 275 to larger perturbation, with perturbations in the range of 80-100% in the parameters still resulting
 276 in predictions with less than 30% median error.

277 We now turn to the question of alignment between different sources of perturbation. From
 278 the results in *Appendix B*, we know that the sensitivity vectors \bar{s}_{u_i} and $\bar{s}_{\theta_{ij}}$ are aligned for any
 279 given i , and for all j . This means that perturbing the environmental parameter u_i or perturbing
 280 any of the elements in the i -th row of Θ will result in changes in the phenotypes in the same
 281 direction. To test this, we generated 100 random reference networks. For each of these reference
 282 networks, we introduced genetic and environmental perturbations, in the first row of the reference

283 Θ^* and in u_1 , respectively. We then simulated the networks until the steady state was reached,
284 and measured the angles between the phenotypic effects of different origins. Figure 3.b. shows that
285 the angles between the vectors resulting from these perturbations are significantly smaller than
286 the angles between random vectors. This confirms that the phenotypic effects of these genetic and
287 environmental perturbations are aligned.

288 *Plasticity and evolvability*

289 The alignment between the phenotypic effects of genetic and environmental perturbations provides a
290 link between plasticity and evolvability. Indeed, the plastic response of organisms to environmental
291 change can be used to infer what variation can arise through heritable genetic changes, and thus
292 what variation can selection act on.

293 To study this, we use populations of individuals represented by gene regulatory networks of 5
294 genes, where only genes 1 and 2 receive environmental input (i.e., $u_3 = u_4 = u_5 = 0$). We have two
295 sets of 15 populations each that we call *up-down* and *left-right* sets, which differ in how organisms
296 respond plastically to environmental perturbation. Figure 4.a shows one example population from
297 the *up-down* set in black, and one example population from the *left-right* population in orange. The
298 dots represent the steady-states of the phenotypes for the individuals when no environmental input
299 is introduced. The arrows have their origin in these unperturbed reference states, and point in the
300 direction of change when environmental perturbations are introduced. The population plotted in
301 black show large changes in x_4 (i.e., the expression level of gene 4) in response to environmental
302 perturbations, but little change in x_3 . The opposite applies to the orange population, which mostly
303 varies in x_3 when environmental perturbations are introduced. Details of how the population sets
304 were generated are given in *Materials and Methods*.

305 Because we know from the analytical results above that the response to environmental perturba-
306 tions is aligned with the response to genetic perturbations, we predict that the *left-right* populations
307 should evolve faster, compared to the *up-down* populations, if selected in the direction of increase
308 in x_3 and no change in x_4 . We test this by making the populations evolve “to the right”, towards

309 an optimum in $(x_3, x_4) = (12.5, 7.5)$. To avoid confounding effects of standing genetic variation,
310 we sampled 25 random individuals from each of the 30 populations (15 *left-right* and 15 *up-down*),
311 and created independent evolutionary lines from 1000 clones of those randomly sampled individuals
312 (i.e., total of $2 \times 15 \times 25 = 750$ independent evolutionary simulations starting from 1000 clones
313 each).

314 Panel 4.b confirms that the individuals from the *left-right* populations are consistently faster at
315 evolving “towards the right”, to an optimum in $(x_3, x_4) = (12.5, 7.5)$, compared to the individuals
316 from the *up-down* populations. The 15 transparent orange lines correspond to the average of
317 the 25 simulations from each of the 15 *left-right* populations. Similarly, the transparent black lines
318 represent the averages from the 15 *up-down* populations. Total averages are given with fully opaque
319 colors.

320 For this particular system, we can further use the sensitivity vectors discovered in the previous
321 section to accelerate evolution in a desired direction. From the analytical results, and as confirmed
322 with the simulations (Figure 3.b.), we know that the i -th environmental input will be aligned with
323 mutations in the i -th row of Θ . Furthermore, we know that the plastic response shown in Figure
324 4.a. is generated by perturbation in u_1 and u_2 . Therefore, we know that evolution in the desired
325 direction can be accelerated by increasing the mutation rate of the first two rows of Θ .

326 Figure 4.c shows a scenario in which additional mutations are introduced in each generation,
327 but only on the first two rows of Θ . For individuals in set *left-right*, many of these mutations will
328 be beneficial since they will be aligned with the plastic response, which itself points towards the
329 optimum at $(x_3, x_4) = (12.5, 7.5)$, as shown in Figure 4.a. This results in a marked acceleration of
330 evolution towards the optimum (compare orange lines in panels b and c of Figure 4). Populations
331 from the set *up-down*, however, cannot benefit from this additional mutational input since we
332 know from Figure 3.c. that mutations in the first two rows of Θ result in phenotypic changes that
333 do not point towards the optimum for the *up-down* populations. Supplementary Figure 2 shows
334 that, analogously, the *up-down* populations out-compete the *left-right* populations if selection is
335 “upwards”, towards an optimum in $(x_3, x_4) = (7.5, 12.5)$, and that evolution is accelerated in this

336 direction if we increase the mutational input in the first two rows of Θ for the *up-down*, but not
337 the *left-right* population.

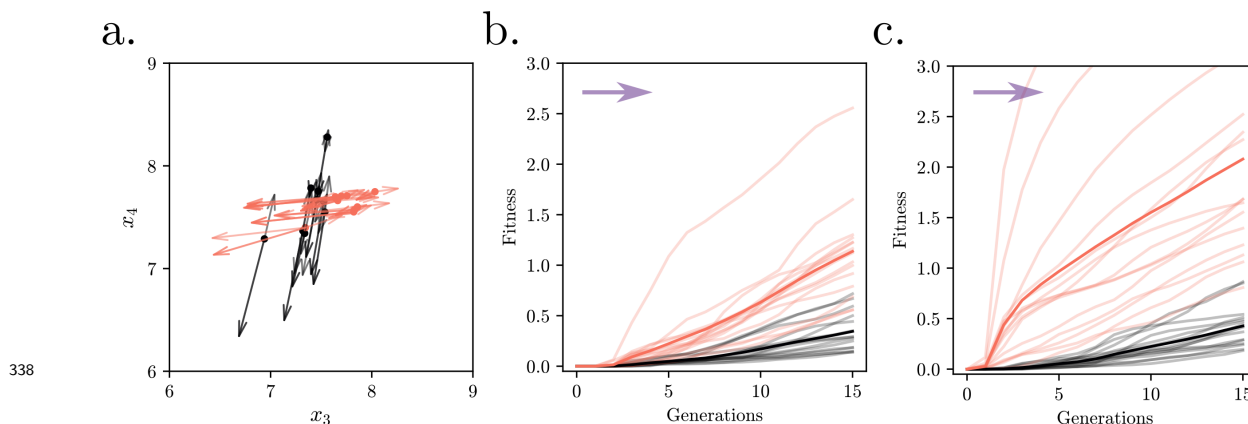


Figure 4: Plasticity predicts evolvability and this can be used for evolutionary control. Panel a. shows an example population of the *left-right* and *up-down* sets, in orange and black respectively. Dots represent unperturbed individuals (no environmental inputs), and the arrows represent the direction of the change in steady states when an environmental perturbation is introduced in one of the first two states. Panel b. shows evolution for *left-right* and *up-down* populations, towards an optimum located in $(x_3, x_4) = (12.5, 7.5)$ represented with the purple arrow. The *left-right* populations, in orange, out-compete the *up-down*. Transparent lines are the average among the 25 evolutionary lines initiated from a single individual from each of the 15 populations in each set. Panel c. shows that an additional mutational input directly on the first two rows of Θ significantly accelerates evolution towards the optimum for the *left-right* populations.

339 Discussion

340 In this work, we demonstrate that representing development as a dynamical system provides a
341 theoretical framework to study how generative processes create phenotypic variation, and thus
342 constrain or facilitate adaptive change. This general representation of development captures two
343 general features of generative processes that are lost in static representations that only focus on
344 the outcome of development, but not on how that outcome is constructed (e.g., static maps from
345 genotypes and environments to adult phenotypes). The first property is historicity, which means
346 that the phenotype at any given time is both the effect of earlier, and the cause of later, develop-
347 mental change. The second property is that all perturbations are ultimately funneled by the same
348 developmental process. These two generic features of development are reflected in the elements of
349 the sensitivity vectors, which determine how the phenotype is expected to change as a result of a

350 perturbation during development.

351 A benefit of this representation of development as a dynamical system is that it establishes
352 a formal connection between plasticity and evolvability, understood as the capacity to generate
353 phenotypic variation in response to perturbations of environmental or genetic origin, respectively.
354 The existence of theoretical conditions for when genetic and environmental perturbations result in
355 concordant phenotypic effects indicates that both phenomena ought to be more broadly concep-
356 tualized as variational properties that reflect the internal structure of the developmental process
357 (Wagner and Altenberg 1996, Salazar-Ciudad 2006). This conceptualization has important impli-
358 cations for evolutionary prediction and control, since it suggests that information of plasticity can
359 reveal salient aspects of evolvability, and vice versa. While this link between plasticity and evolv-
360 ability has been demonstrated before in specific models (Ancel and Fontana 2000, Espinosa-Soto
361 et al. 2011, Draghi and Whitlock 2012, van Gestel and Weissing 2016, Brun-Usan et al. 2021), the
362 framework presented here extends this understanding in multiple ways.

363 First, the general framework based on sensitivity functions allows defining explicit theoretical
364 conditions for when plasticity and evolvability should be aligned. These conditions are general
365 and apply to any system of the general form of equation (1), since they are derived from generic
366 features of development represented as a process. Due to their generality, these conditions open
367 the possibility to scale these results for application in evolutionary prediction and control in diverse
368 systems. Importantly, these conditions apply to any point during development and are not con-
369 strained to be applied to the adult. This can be important if, for example, selection occurs during
370 development. A limitation for applying this framework to phenotypic variation in nature is that
371 the developmental function \mathbf{f} needs to be known to calculate matrix $A(t)$ and vector $b(t)$. Note
372 however that even if we cannot obtain explicit analytical values for these elements, the general
373 conclusions of the framework still apply. Furthermore, there is potential to estimate the sensitivity
374 functions directly from data when the developmental function is not known (e.g., by analyzing the
375 phenotypic consequences of experimental perturbations, Milocco and Uller 2023).

376 Second, the framework makes it possible to go beyond the qualitative expectation that genetic

377 and environmental perturbations are interchangeable in development (e.g., Cheverud 1982, 1988;
378 West-Eberhard 2003), by making quantitative predictions of the phenotypic effect of perturbation,
379 and of the relationship between different perturbations. As shown in this paper, this information
380 can be exploited to predict responses to selection without an estimate of heritable (co)variance
381 in phenotypes (e.g., as summarized in the G matrix). This is possible because knowledge about
382 plasticity captures properties of developmental systems that carries information about how those
383 systems can accumulate heritable phenotypic variation. While some empirical data (e.g., Noble et
384 al. 2019) could be interpreted in this manner, there appears to be no direct test of this prediction.
385 Note, however, that the framework introduced here is only locally valid, meaning that it is predictive
386 of the effects of perturbations of small size. Therefore, predictions of evolvability based on plasticity
387 may only be valid for a limited number of generations after which the sensitivity functions would
388 have to be re-identified since the internal structure of development may have changed.

389 Finally, the framework reveals how to exploit this alignment for evolutionary control, by accel-
390 erating evolution in certain directions through forced mutations predicted to result in adaptive phe-
391 notypic changes. More generally, if the sensitivity vectors of multiple perturbations are identified,
392 this means that it is possible to design combinations of perturbations to drive the developmental
393 process in a desired direction. Similar to the other points above, this insight suggests opportunities
394 for empirical investigation of evolvability, which also may have implications in applied fields of
395 biology such as biotechnology.

396 While so far we have emphasized the alignment between the phenotypic effects of genetic and
397 environmental perturbations, different genetic perturbations can also be aligned with each other
398 (Pitchers et al. 2019). In the simulations, this redundancy is evidenced by the fact that mutating
399 any element of the i -th row of Θ in the gene regulatory network or mutating any of the parameters
400 k or F in the reaction-diffusion model, generates concordant phenotypic change. In this way, a
401 population will evolve in the same direction of trait space by accumulating mutations in any of
402 those equivalent elements. This redundancy can explain why genetic changes underlying parallel
403 evolution often fail to be replicated (e.g., Pelletier et al. 2023), since multiple changes at the genetic

404 level can explain the same phenotypic adaptations.

405 Redundancy ultimately reflects the fact that it is not the identity of any specific gene that
406 matters for the generation of phenotypic variation, but rather the role it plays in the dynamics of
407 the developmental process. This can explain the observation that, despite the multidimensional
408 nature of phenotypic data, it is very often the case that there are only a few effective dimensions
409 of variation (Beldade et al. 2002, Houle et al. 2016, Alba et al. 2021, Rohner and Berger 2023).
410 Indeed, if many perturbations result in concordant phenotypic changes, then phenotypic variation
411 will be restricted to a manifold of lower dimension than the total number phenotypic variables.

412 Following this, we should expect that parallel evolution will be explained by a repeatable genetic
413 change only in cases where the effect of perturbing that gene is unaligned with others (i.e., the
414 associated vector $\tilde{\mathbf{b}}_\lambda$ in equation (5) is unique). This represents a scenario where the perturbed
415 gene plays a distinctive role in developmental dynamics. One possible example of this is the gain and
416 loss of red and yellow carotenoid coloration in diverse vertebrates (e.g., birds, mammals, lizards),
417 which is commonly associated with perturbations in the expression of gene *BCO2* that encodes a
418 carotenoid degradation enzyme (Våge and Boman 2010, Andrade et al. 2019). This evidence implies
419 that *BCO2* plays a distinctive role in the generation of color, so that perturbations in its functioning
420 have distinctive phenotypic effects. Repeatable genetic changes underlying parallel evolution can
421 thus be used to make inferences about developmental dynamics, guiding future research.

422 Conclusion

423 An understanding of evolution is incomplete without a theory of how phenotypic variation is gen-
424 erated in each generation. The representation of development as a process provides the conceptual
425 basis to predict when perturbations of different origins result in similar phenotypic changes. Our
426 results indicate that a promising avenue for future research on the generation of variation will not
427 focus on the specific identity of elements such as genes, but rather focus on how those elements
428 participate in a dynamical process that integrates different sources of information to produce phe-

429 notypes.

430 **Materials and Methods**

431 **Reaction-diffusion simulations**

432 The tissue is composed of a grid of 50×50 cells, each having a given amount of the two
433 morphogens, thus resulting in a total of 5000 states. Diffusion occurs only between neighboring
434 cells and is represented with a discretized version of the Laplacian as commonly done (e.g., Sick
435 et al. 2006). Periodic boundary conditions are assumed, so the tissue can be thought of as being
436 mapped to a torus. The first 2500 states are the concentration of morphogen 1 in the 2500 cells,
437 while the last 2500 states correspond to the concentration of morphogen 2. This means that for
438 $i = 1, 2, \dots, 2500$, x_i corresponds to concentration of morphogen 1 of the cell located in position
439 $(q + 1, r)$ of the grid where q and r are the quotient and remainder, respectively, of the division
440 $i \div 50$, where \div represents integer division. Similarly, x_i for $i = 2501, 2502, \dots, 5000$ corresponds
441 to the concentration of morphogen 2 of the cell located in position $(q + 1, r)$ of the grid where q
442 and r are the quotient and remainder, respectively, of the division $(i - 2500) \div 50$. To obtain the
443 sensitivity vectors, we need the Jacobian and the weights. These are obtained by differentiating the
444 discretized equation. The Jacobian results in a sparse matrix since only neighboring cells interact
445 (through diffusion). The Jacobian and the weights are given in the accompanying scripts.

446 **Populations of gene-regulatory networks** To generate the *up-down* and *left-right* pop-
447 ulations, composed of individuals that have plastic responses in different directions, we evolve
448 populations under fluctuating selection tracking an optimum with a correlated environmental in-
449 put (see Draghi and Whitlock 2012). Specifically, in each generation, the position of the optimum
450 is correlated with the environmental inputs, so the networks with higher fitness are those that allow
451 individuals to track the optimum in each generation using the environmental input. To simplify
452 the figures, out of the 5 genes, only genes 1 and 2 receive environmental input and selection acts
453 only on genes 3 and 4. We evolve the populations for 500 generations, starting with 1000 clones
454 that were randomly generated. All optimums fluctuated around a value of $(x_3, x_4) = (7.5, 7.5)$. A
455 set of 15 populations were evolved to track an optimum that fluctuated for values of x_3 around 7.5,

456 but keeping x_4 fixed at 7.5. We refer to this first set of populations as *left-right*. Another set of 15
457 populations, which we refer to as *up-down*, evolved tracking an optimum where x_4 fluctuated and
458 x_3 was fixed at 7.5.

459 **Angle between sensitivity vectors** The angle $\theta(t)$ between the directions of two sensitivity
460 vectors $\mathbf{s}_{\lambda_1}(t)$ and $\mathbf{s}_{\lambda_2}(t)$ is defined as the minimum between the angle formed by $\mathbf{s}_{\lambda_1}(t)$ and $\mathbf{s}_{\lambda_2}(t)$,
461 and the angle formed by $-\mathbf{s}_{\lambda_1}(t)$ and $\mathbf{s}_{\lambda_2}(t)$. By taking the minimum we make sure that $\theta(t)$
462 depends on the direction of the vectors and not the sign. Complete alignment between $\mathbf{s}_{\lambda_1}(t)$
463 and $\mathbf{s}_{\lambda_2}(t)$ is then given by $\theta(t) = 0^\circ$, in which case the sensitivity vectors have the exact same
464 direction (but possibly different signs). This will be the case if the weights are proportional (i.e.,
465 $\tilde{\mathbf{b}}_{\lambda_1}(t, \boldsymbol{\lambda}^*) = \alpha \tilde{\mathbf{b}}_{\lambda_2}(t, \boldsymbol{\lambda}^*)$ with α constant). More generally, however, we consider that there is
466 evidence for alignment if the angle $\theta(t)$ is significantly smaller, at a given confidence level, than
467 the distribution of angles between independent random vectors in \mathbb{R}^n , with n being the number of
468 states. We note that as n becomes larger, the distribution of angles between random vectors in \mathbb{R}^n
469 concentrates around 90° , so random vectors are generally 'more' orthogonal in higher dimensional
470 spaces. In this way, $\theta(t) < 90^\circ$ in higher dimensions is a signature of alignment.

471 Appendixes

472 Appendix A

473 Here, we obtain an expression for the sensitivity vectors. We begin with the general representation
 474 of development as a dynamical system, as given by equation (1). Under the assumption that the
 475 developmental function \mathbf{f} is smooth, there exists a unique solution $\mathbf{x}(t, \lambda)$ for a λ close to the
 476 reference value λ^* , which can be obtained as (see Khalil 2002)

$$\mathbf{x}(t, \lambda) = \mathbf{x}_0 + \int_{t_0}^t \mathbf{f}(\tau, \mathbf{x}(\tau, \lambda), \lambda) d\tau \quad (\text{A1})$$

477 We are interested in calculating the sensitivity vector, as defined in equation (2). For this, we
 478 take the partial derivative with respect to λ on both sides of equation (A1), which gives

$$\begin{aligned} \mathbf{s}_\lambda(t) &= \frac{\partial \mathbf{x}(t, \lambda)}{\partial \lambda} = \frac{\partial}{\partial \lambda} \left[\mathbf{x}_0 + \int_{t_0}^t \mathbf{f}(\tau, \mathbf{x}(\tau, \lambda), \lambda) d\tau \right] \\ &= \int_{t_0}^t \left[\frac{\partial \mathbf{f}(\tau, \mathbf{x}(\tau, \lambda), \lambda)}{\partial \mathbf{x}(\tau, \lambda)} \mathbf{s}_\lambda(\tau) + \frac{\partial \mathbf{f}(\tau, \mathbf{x}(\tau, \lambda), \lambda)}{\partial \lambda} \right] d\tau \end{aligned} \quad (\text{A2})$$

479 where we use that the derivative of the integral is equal to the integral of the derivative, and
 480 that the derivative of the initial condition is zero because it does not depend on λ . We further use
 481 the chain rule to obtain the derivative of \mathbf{f} with respect to λ .

482 To obtain an expression of how the sensitivity vector changes in time, we take the partial
 483 derivative of the equation (A2) with respect to time, yielding equation (4).

484 Appendix B

485 Here, we derive the equations for the Jacobian, weights and sensitivity vectors for the developmental
 486 parameters of the gene regulatory network. We begin by rewriting equation (7) in matrix form.
 487 For this, we write $\mathbf{h} = \Theta \mathbf{x} + \mathbf{u}$, and define $\boldsymbol{\kappa} = (K_1, K_2, \dots, K_n)$ and the $n \times n$ diagonal matrix
 488 $M = \text{diag}(\mu_1, \mu_2, \dots, \mu_n)$. This yields

$$\dot{\mathbf{x}} = \mathbf{f}(t, \mathbf{x}, \Theta, \mathbf{u}, M, \boldsymbol{\kappa}) = R(\mathbf{h}) - M\mathbf{x} \quad \text{with} \quad R(\mathbf{h}) = \begin{pmatrix} \frac{r(h_1)}{K_1 + r(h_1)} \\ \vdots \\ \frac{r(h_n)}{K_n + r(h_n)} \end{pmatrix} \quad (\text{A3})$$

489 which follows the form of equation (1), with the developmental parameter vector given by $\boldsymbol{\lambda} =$
 490 $(\Theta, \mathbf{u}, M, \boldsymbol{\kappa})$ and reference developmental parameter values given in the vector $\boldsymbol{\lambda}^* = (\Theta^*, \mathbf{u}^*, M^*, \boldsymbol{\kappa}^*)$.

491 The study of alignment in this example is performed at the steady state, with $\dot{x}_i = 0$ for all
 492 i . We therefore assume that the reference values for the developmental parameters, given by $\boldsymbol{\lambda}^*$,
 493 result in a stable system able to reach a steady state. Further, we assume that $\bar{h}_i > 0$, with the bar
 494 indicating the steady state. This allows to replace $r(\bar{h}_i) = \bar{h}_i$. Note that if $\bar{h}_i < 0$, then equation (7)
 495 reduces to $\dot{x}_i = -\mu_i x_i$ and it can be easily checked that this results in $\bar{\mathbf{b}}_{u_i} = \bar{\mathbf{b}}_{\theta_{ij}} = \bar{\mathbf{b}}_{\mu_i} = \bar{\mathbf{b}}_{K_i} = \mathbf{0}$.

496 In other words, the steady state is robust to perturbations in the developmental parameters if
 497 $\bar{h}_i < 0$.

498 We obtain the Jacobian,

$$499 \quad \bar{A} = \frac{\partial \mathbf{f}}{\partial \mathbf{x}} \Big|_{\bar{\mathbf{x}}, \lambda^*} = \frac{\partial \mathbf{f}}{\partial \mathbf{h}} \frac{\partial \mathbf{h}}{\partial \mathbf{x}} \Big|_{\bar{\mathbf{x}}, \lambda^*} - M^* = \begin{pmatrix} \bar{\alpha}_1 & \dots & 0 \\ \vdots & \ddots & \vdots \\ 0 & \dots & \bar{\alpha}_n \end{pmatrix} \Theta^* - M^* \quad (\text{A4})$$

500 where the bars indicate variables in the steady state, asterisks indicate reference value, and $\bar{\alpha}_i =$
 501 $K_i/(K_i + \bar{h}_i)^2$. We now calculate the weights $\bar{\mathbf{b}}_\lambda$ as

$$502 \quad \bar{\mathbf{b}}_{u_i} = \frac{\partial \mathbf{f}}{\partial u_i} \Big|_{\bar{\mathbf{x}}, \lambda^*} = \frac{\partial \mathbf{f}}{\partial \mathbf{h}} \frac{\partial \mathbf{h}}{\partial u_i} \Big|_{\bar{\mathbf{x}}, \lambda^*} = \begin{pmatrix} \vdots \\ 0 \\ \bar{\alpha}_i \\ 0 \\ \vdots \end{pmatrix}, \quad \bar{\mathbf{b}}_{K_i} = \frac{\partial \mathbf{f}}{\partial K_i} \Big|_{\bar{\mathbf{x}}, \lambda^*} = \begin{pmatrix} \vdots \\ 0 \\ \bar{\gamma}_i \\ 0 \\ \vdots \end{pmatrix},$$

$$503 \quad \bar{\mathbf{b}}_{\mu_i} = \frac{\partial \mathbf{f}}{\partial \mu_i} \Big|_{\bar{\mathbf{x}}, \lambda^*} = \begin{pmatrix} \vdots \\ 0 \\ \bar{x}_i \\ 0 \\ \vdots \end{pmatrix}, \quad \bar{\mathbf{b}}_{\theta_{ij}} = \frac{\partial \mathbf{f}}{\partial \theta_{ij}} \Big|_{\bar{\mathbf{x}}, \lambda^*} = \frac{\partial \mathbf{f}}{\partial \mathbf{h}} \frac{\partial \mathbf{h}}{\partial \theta_{ij}} \Big|_{\bar{\mathbf{x}}, \lambda^*} = \begin{pmatrix} \vdots \\ 0 \\ \bar{\alpha}_i \bar{x}_j \\ 0 \\ \vdots \end{pmatrix},$$

504
 505 with $\bar{\gamma}_i = -\bar{h}_i/(K_i + \bar{h}_i)$. Because the Jacobian is invertible, we can obtain the sensitivity vectors
 506 with the simplified expression given in equation (5), as

$$507 \quad \bar{\mathbf{s}}_{u_i} = -\bar{A}^{-1} \bar{\mathbf{b}}_{u_i}, \quad \bar{\mathbf{s}}_{\theta_{ij}} = -\bar{A}^{-1} \bar{\mathbf{b}}_{\theta_{ij}}, \quad \bar{\mathbf{s}}_{\mu_i} = -\bar{A}^{-1} \bar{\mathbf{b}}_{\mu_i}, \quad \bar{\mathbf{s}}_{K_i} = -\bar{A}^{-1} \bar{\mathbf{b}}_{K_i}. \quad (\text{A5})$$

508 Thus, the sensitivity functions for u_i , θ_{ij} , μ_i , and K_i are always aligned for a given i and all j .
 509 In particular, they point in the direction of the i -th column of \bar{A}^{-1} .

510 References

- 511 1. Alba, V., Carthew, J. E., Carthew, R. W., & Mani, M. (2021). Global constraints within the
512 developmental program of the *Drosophila* wing. *Elife*, 10, e66750.
- 513 2. Alberch, P. (1991). From genes to phenotype: dynamical systems and evolvability. *Genetica*,
514 84(1), 5-11.
- 515 3. Ancel, L. W., & Fontana, W. (2000). Plasticity, evolvability, and modularity in RNA. *Journal*
516 *of Experimental Zoology*, 288(3), 242-283.
- 517 4. Andrade, P., Pinho, C., Pérez i de Lanuza, G., Afonso, S., Brejcha, J., Rubin, C. J., ... &
518 Carneiro, M. (2019). Regulatory changes in pterin and carotenoid genes underlie balanced
519 color polymorphisms in the wall lizard. *Proceedings of the National Academy of Sciences*,
520 116(12), 5633-5642.
- 521 5. Bassett, E. A., & Wallace, V. A. (2012). Cell fate determination in the vertebrate retina.
522 *Trends in neurosciences*, 35(9), 565-573.
- 523 6. Beldade, P., Koops, K., & Brakefield, P. M. (2002). Developmental constraints versus flexi-
524 bility in morphological evolution. *Nature*, 416(6883), 844-847.
- 525 7. Brakefield, P. M. (2006). Evo-devo and constraints on selection. *Trends in Ecology & Evolu-*
526 *tion*, 21(7), 362-368.
- 527 8. Brun-Usan, M., Rago, A., Thies, C., Uller, T., & Watson, R. A. (2021). Development
528 and selective grain make plasticity'take the lead'in adaptive evolution. *BMC Ecology and*
529 *Evolution*, 21(1), 1-17.
- 530 9. Burggren, W. W., & Mueller, C. A. (2015). Developmental critical windows and sensitive
531 periods as three-dimensional constructs in time and space. *Physiological and Biochemical*
532 *Zoology*, 88(2), 91-102.
- 533 10. Cheverud, J. M. (1982). Phenotypic, genetic, and environmental morphological integration
534 in the cranium. *Evolution*, 499-516.
- 535 11. Cheverud, J. M. (1988). A comparison of genetic and phenotypic correlations. *Evolution*,
536 42(5), 958-968.
- 537 12. Chevin, L. M., Leung, C., Le Rouzic, A., & Uller, T. (2022). Using phenotypic plasticity to
538 understand the structure and evolution of the genotype–phenotype map. *Genetica*, 150(3-4),
539 209-221.
- 540 13. Draghi, J. A., & Whitlock, M. C. (2012). Phenotypic plasticity facilitates mutational variance,
541 genetic variance, and evolvability along the major axis of environmental variation. *Evolution*,
542 66(9), 2891-2902.
- 543 14. Espinosa-Soto, C., Martin, O. C., & Wagner, A. (2011). Phenotypic plasticity can facilitate
544 adaptive evolution in gene regulatory circuits. *BMC evolutionary biology*, 11, 1-14.

- 545 15. Furusawa, C., & Kaneko, K. (2015). Global relationships in fluctuation and response in
546 adaptive evolution. *Journal of The Royal Society Interface*, 12(109), 20150482.
- 547 16. Galis, F., Arntzen, J. W., & Lande, R. (2010). Dollo's law and the irreversibility of digit loss
548 in *Bachia*. *Evolution*, 64(8), 2466-2476.
- 549 17. Gilbert S. F. and Barresi M. J. F. (2016). Developmental biology. Sunderland, MA: *Sinauer*
550 *Associates*.
- 551 18. González-Forero, M. (2023). How development affects evolution. *Evolution*, 77(2), 562-579.
- 552 19. Gray, P., & Scott, S. K. (1990). Archetypal response patterns for open chemical systems
553 with two components. *Philosophical Transactions of the Royal Society of London. Series A:*
554 *Physical and Engineering Sciences*, 332(1624), 69-87.
- 555 20. Green, J. B., & Sharpe, J. (2015). Positional information and reaction-diffusion: two big
556 ideas in developmental biology combine. *Development*, 142(7), 1203-1211.
- 557 21. Houle, D., Bolstad, G. H., van der Linde, K., & Hansen, T. F. (2017). Mutation predicts 40
558 million years of fly wing evolution. *Nature*, 548(7668), 447-450.
- 559 22. Khalil, H.K. (2002). Nonlinear Systems. Pearson Education, 3rd edition.
- 560 23. Kirschner, M., & Gerhart, J. (1998). Evolvability. *Proceedings of the National Academy of*
561 *Sciences*, 95(15), 8420-8427.
- 562 24. Kondo, S., & Miura, T. (2010). Reaction-diffusion model as a framework for understanding
563 biological pattern formation. *Science*, 329(5999), 1616-1620.
- 564 25. Lewontin, R. C. (1983). The organism as the subject and object of evolution. *Scientia*,
565 77(18).
- 566 26. Lynch, M., & Walsh, B. (1998). Genetics and analysis of quantitative traits. *Sinauer Asso-*
567 *ciates*, Sunderland, MA.
- 568 27. Milocco, L., & Uller, T. (2023). A data-driven framework to model the organism–environment
569 system. *Evolution & Development*.
- 570 28. Morrissey, M. B. (2015). Evolutionary quantitative genetics of nonlinear developmental sys-
571 tems. *Evolution*, 69:2050–2066.
- 572 29. Nijhout, H. F. (1984). Colour pattern modification by coldshock in Lepidoptera. *Develop-*
573 *ment*, 81(1), 287-305.
- 574 30. Noble, D. W., Radersma, R., & Uller, T. (2019). Plastic responses to novel environments are
575 biased towards phenotype dimensions with high additive genetic variation. *Proceedings of the*
576 *National Academy of Sciences*, 116(27), 13452-13461.
- 577 31. Pelletier, K., Pitchers, W. R., Mammel, A., Northrop-Albrecht, E., Márquez, E. J., Moscarella,
578 R. A., Houle, D. & Dworkin, I. (2023). Complexities of recapitulating polygenic effects in
579 natural populations: replication of genetic effects on wing shape in artificially selected and
580 wild-caught populations of *Drosophila melanogaster*. *Genetics*, Volume 224, Issue 3.

- 581 32. Pearson, J. E. (1993). Complex patterns in a simple system. *Science*, 261(5118), 189-192.
- 582 33. Pitchers, W., Nye, J., Márquez, E. J., Kowalski, A., Dworkin, I., & Houle, D. (2019). A mul-
583 tivariate genome-wide association study of wing shape in *Drosophila melanogaster*. *Genetics*,
584 211(4), 1429-1447.
- 585 34. Rice, S. H. (2002). A general population genetic theory for the evolution of developmental
586 interactions. *Proceedings of the National Academy of Sciences*, 99(24), 15518-15523.
- 587 35. Rohner, P. T., & Berger, D. (2023). Developmental bias predicts 60 million years of wing
588 shape evolution. *Proceedings of the National Academy of Sciences*, 120(19), e2211210120.
- 589 36. Salazar-Ciudad, I. (2006), Developmental constraints vs. variational properties: how pattern
590 formation can help to understand evolution and development. *J. Exp. Zool.*, 306B: 107-125.
- 591 37. Salazar-Ciudad, I., & Jernvall, J. (2010). A computational model of teeth and the develop-
592 mental origins of morphological variation. *Nature*, 464(7288), 583-586.
- 593 38. Sick, S., Reinker, S., Timmer, J., & Schlake, T. (2006). WNT and DKK determine hair
594 follicle spacing through a reaction-diffusion mechanism. *Science*, 314(5804), 1447-1450.
- 595 39. Stent, G. S. (1985). Thinking in one dimension: the impact of molecular biology on develop-
596 ment. *Cell*, 40(1), 1-2.
- 597 40. Turing, A. M. (1952). The chemical basis of morphogenesis. *Philos. Trans. R. Soc. Lond.*
598 *B Biol. Sci.*, 237, 37-72.
- 599 41. Våge, D. I., & Boman, I. A. (2010). A nonsense mutation in the beta-carotene oxygenase 2
600 (BCO2) gene is tightly associated with accumulation of carotenoids in adipose tissue in sheep
601 (*Ovis aries*). *BMC genetics*, 11(1), 1-6.
- 602 42. van Gestel, J., & Weissing, F. J. (2016). Regulatory mechanisms link phenotypic plasticity
603 to evolvability. *Scientific reports*, 6(1), 24524.
- 604 43. Wagner, A. (1994). Evolution of gene networks by gene duplications: a mathematical model
605 and its implications on genome organization. *Proceedings of the National Academy of Sci-*
606 *ences*, 91(10), 4387-4391.
- 607 44. Wagner, G. P., & Altenberg, L. (1996). Perspective: complex adaptations and the evolution
608 of evolvability. *Evolution*, 50(3), 967-976.
- 609 45. West-Eberhard, M. J. (2003). Developmental plasticity and evolution. *Oxford University*
610 *Press*.

611 **Acknowledgements**

612 The authors thank Ruben H. Milocco for discussion. The authors thank the John Templeton
613 Foundation (62220) for financial support. The opinions expressed in this paper are those of the
614 authors and not those of the John Templeton Foundation.

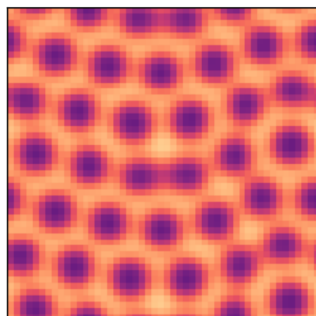
615 **Competing interests**

616 The authors declare no competing interests.

617 **Data availability**

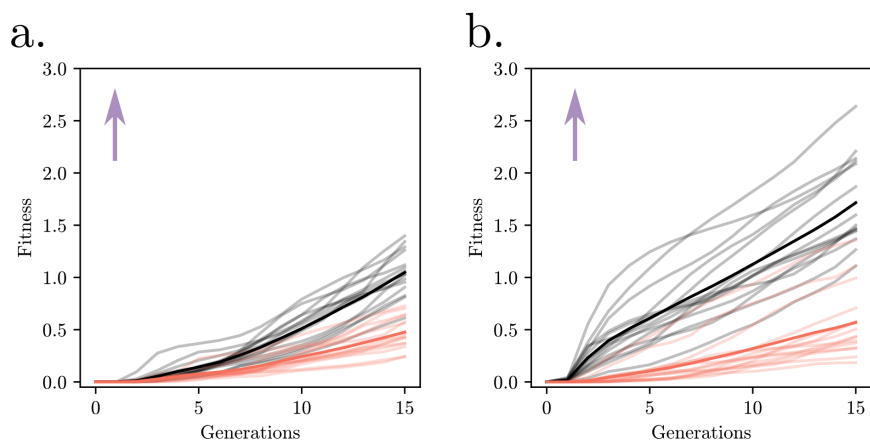
618 The *Python* scripts for the reaction-diffusion and gene regulatory network simulations and analyses
619 will be uploaded to <https://github.com/lisandromilocco>.

620 Supplementary Figures



Initial condition

621 **Supplementary Figure 1.** Initial conditions for the reaction-diffusion simulations.



622 **Supplementary Figure 2.** This figure is analogous to Main Figure 4 but for selection "upwards",
623 towards an optimum in $(x_3, x_4) = (7.5, 12.5)$ as represented by the purple arrow. Panel a. shows
624 evolution for *left-right* and *up-down* populations, in orange and black respectively. The *up-down*
625 populations out-compete the *left-right*, as expected from their plastic responses shown in Main
626 Figure 4.a. Transparent lines are the average among the 25 evolutionary lines initiated from a
627 single individual from each of the 15 populations in each set. Panel b. shows that an additional
628 mutational input directly on the first two rows of Θ significantly accelerates evolution towards the
629 optimum for the *up-down* populations.